Construction Materials

ice Publishing

Aerial additive building manufacturing: three-dimensional printing of polymer structures using drones

Barrie Dams MEng
PhD Research Student, BRE Centre for Innovative Construction Materials,
Department of Architecture & Civil Engineering, University of Bath, Bath,
UK (corresponding author: b.dams@bath.ac.uk)
(Orcid:0000-0001-7081-5457)

Sina Sareh BSc, MSc, PhD
Academic Leader in Robotics, School of Design, Royal College of Art,
London, UK (Orcid:0000-0002-9787-1798)

Ketao Zhang BSc, PhD
Research Associate, Aerial Robotics Laboratory, Department of Aeronautics,
Imperial College London, London, UK (Orcid:0000-0002-6033-071X)

Paul Shepherd MA, PhD, PGCAPP, CSci, CMath, CEng, MICE,
FIMA, SFHEA
Senior Lecturer, Centre for Advanced Studies in Architecture, Department
of Architecture & Civil Engineering, University of Bath, Bath, UK
(Orcid:0000-0001-7078-4232)

Mirko Kovac MSc, PhD
Director, Aerial Robotics Laboratory; Senior Lecturer, Department of
Aeronautics, Imperial College London, London, UK
(Orcid:0000-0002-9720-2463)

Richard J. Ball BEng, PhD, FHEA, CSci, CEng, FIMMM
Reader, BRE Centre for Innovative Construction Materials, Department of
Architecture & Civil Engineering, University of Bath, Bath, UK
(Orcid:0000-0002-7413-3944)

This paper describes the first aerial additive building manufacturing system developed to create and repair civil engineering structures remotely using polymers extruded from unmanned aerial robots (drones). The structural potential of three commercially available expanding polyurethane foams of varying density (LD40, Reprocell 300 and Reprocell 500), and their feasibility for deposition using an autonomous flying dual-syringe device is described. Test specimens consisting of one and two layers, with horizontal and vertical interfaces, were mechanically tested both parallel and perpendicular to the direction of expansion. LD40 specimens exhibited ductile failure in flexural tests and provided evidence that the interfaces between layers were not necessarily regions of weaknesses. Hand-mixed specimens of Reprocell 500 possessed compressive strengths comparable to those of concrete and flexural strengths similar to those of the lower range of timber, though they exhibited brittle failure. There are challenges to be faced with matching the performance of hand-mixed specimens using an autonomous dual-syringe deposition device, primarily concerning the rheological properties of the material following extrusion. However, the device successfully imported and deposited two liquid components, of varying viscosity, and maintained correct mixing ratios. This work has demonstrated the structural and operational feasibility of polyurethane foam as a viable structural material for remote three-dimensional printing using drones.

1. Introduction

Additive manufacturing in the construction industry currently consists of large, ground-based processes (Kreiger *et al.*, 2015; Lim *et al.*, 2012) that are reliant upon favourable topography, soil conditions and climate. The size of an additive-manufactured, or '3D printed', building is restricted by the size of the deposition machinery. Structures have been created without the need for formwork, using both cementitious materials with contour crafting, concrete printing and D-shape printing methods (Labonnote *et al.*, 2016; Le *et al.*, 2012; Lim *et al.*, 2012), and polymeric materials, an example of which is the 'canal house' in Amsterdam, which consists of bio-plastic elements (Frearson, 2016; Labonnote *et al.*, 2016). Additive manufacturing technologies currently being investigated for applications in the construction industry broadly fall into three categories: fused filament fabrication, powder bed printing and

extrusion printing (Kreiger *et al.*, 2015; Stansbury and Idacavage, 2016). The last method extrudes fluid from a nozzle one layer at a time. The interface between these layers is of critical importance, as factors such as the adhesive, rheological and curing properties of the material, height of layers and speed of deposition all affect the interface and whether it may become an area of weakness in the ensuing structure (Kreiger *et al.*, 2015; Lim *et al.*, 2012).

Aerial robots have been established in a variety of applications including remote sensing (Sugiura *et al.*, 2003a), agriculture (Sugiura *et al.*, 2003b), aerial photography (Schutte *et al.*, 2001) and surveillance (Wright, 2005), and are being considered in other areas such as courier delivery (Siciliano and Khatib, 2008). Within the aerial additive building manufacturing (Aerial ABM) project, it is envisaged that a coordinated

3

Construction Materials
Volume 173 Issue 1

Aerial additive building manufacturing:
three-dimensional printing of polymer
structures using drones
Dams, Sareh, Zhang *et al.*

swarm of aerial robots, each equipped with a three-dimensional (3D) printing device depositing viscous liquid with suitable mechanical properties, can construct or repair buildings free from constraints concerning size, soil conditions and topography. This would be particularly applicable where hazardous or inaccessible environments are involved. The feasibility of 3D printing using a single aerial robot was demonstrated by the co-authors at the Aerial Robotics Laboratory of Imperial College London (Hunt *et al.*, 2014).

This paper investigates the feasibility of autonomous 3D extrusion printing of buildings and infrastructure repair applications using polyurethane foam. Expanding polyurethane foam is established in the construction industry as a method of insulating buildings (Wu *et al.*, 2012) due to its low coefficient of thermal conductivity (Zhang *et al.*, 2014). To the authors' knowledge, expanding polyurethane foam has not previously been used as a structural material in either residential or commercial construction projects. This study compares low-density LD40 foam used for thermal insulation (Isothane, 2016a) with higher density foams Reprocell 300, marketed as a substitute for timber in prop and set design, and Reprocell 500, which is used for deep-sea buoyancy applications (Isothane, 2016b).

A feasibility study of the two low-density polyurethane foam liquid components (Hunt *et al.*, 2014) demonstrated that these liquids could be carried by an aerial robot capable of mixing and extrusion 3D printing the material during controlled, coordinated flight. Quadcopters capable of depositing foam within a defined 10 cm radius circle have been developed (Hunt *et al.*, 2014), and Figure 1 illustrates the robot in flight with an attached, deployed dual-syringe device and a mixing nozzle of preliminary design.

2. Experimental methodology

The mechanical, morphological and rheological properties of the foams were laboratory tested to determine structural and operational feasibility.

2.1 Polyurethane foam

The liquid components of LD40, Reprocell 300 and Reprocell 500 consist of a polyol resin and an isocyanate hardener (Alaa *et al.*, 2015), with the resulting rigid foam a product of polymerisation, as two isocyanate groups per molecule chemically react with the polyol (Trovati *et al.*, 2010). The mixing ratio was 1:1 by volume for all three foams.

Foam specimens were made using three methods.

- 'Cut-edged': pouring liquid components into a tray and hand mixing to create a bulk of material, which was subsequently cut into specimens using an electric band saw.
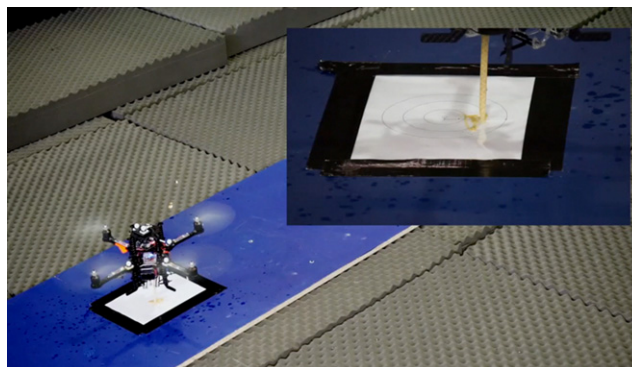

Figure 1. Aerial additive building manufacturing – a 3D printing system on-board an aerial robot capable of depositing foam within a defined 10 cm radius

- 'Moulded': pouring hand-mixed liquid into wooden moulds that had been sealed and pre-sprayed with Macsil releasing agent.
- Deposition of mixed liquid on to a plastic modelling mat by an autonomous, powered dual-syringe device.

It was necessary to determine whether a closed porosity moulded edge provided properties significantly different from those provided by an open porosity cut edge. Test specimens were created both in one cycle of deposition, forming a single layer, and in two deposition cycles, forming either horizontal or vertical interfaces in the material. The interfaces are illustrated in Figure 2, which also shows images of the moulded, one-layer specimens for all three foams created for compressive strength tests.

2.2 Mixing by hand

The Reprocell 500 liquid components required heating to a temperature of 35°C ± 5°C and, once poured together, required constant stirring to cream at 30 ± 10 s due to the isocyanate and polyol resin not initially being entirely miscible. At ≈90 s, the light honey-coloured cream began to change to a darker brown, thinner liquid as the polymerisation process began, resulting in an exothermic reaction increasing the temperature to over 100°C. Expansion occurred at 135 s with the isocyanate reacting with the water in the polyol resin. Pouring took place between 140 and 160 s with solidification at 180 s. Reprocell 300 specimens were created using a similar method; however, the exothermic reaction reached ≈80°C. LD40 required minimal stirring at room temperature to cream, and exothermic reactions below 50°C did not produce a visible change in the creamed liquid colour or viscosity.

LD40 specimens, with an average density of 45 kg/m³, possessed a high expansion ratio of 20:1 during polymerisation. Reprocell

4

Construction Materials
Volume 173 Issue 1

Aerial additive building manufacturing: three-dimensional printing of polymer structures using drones
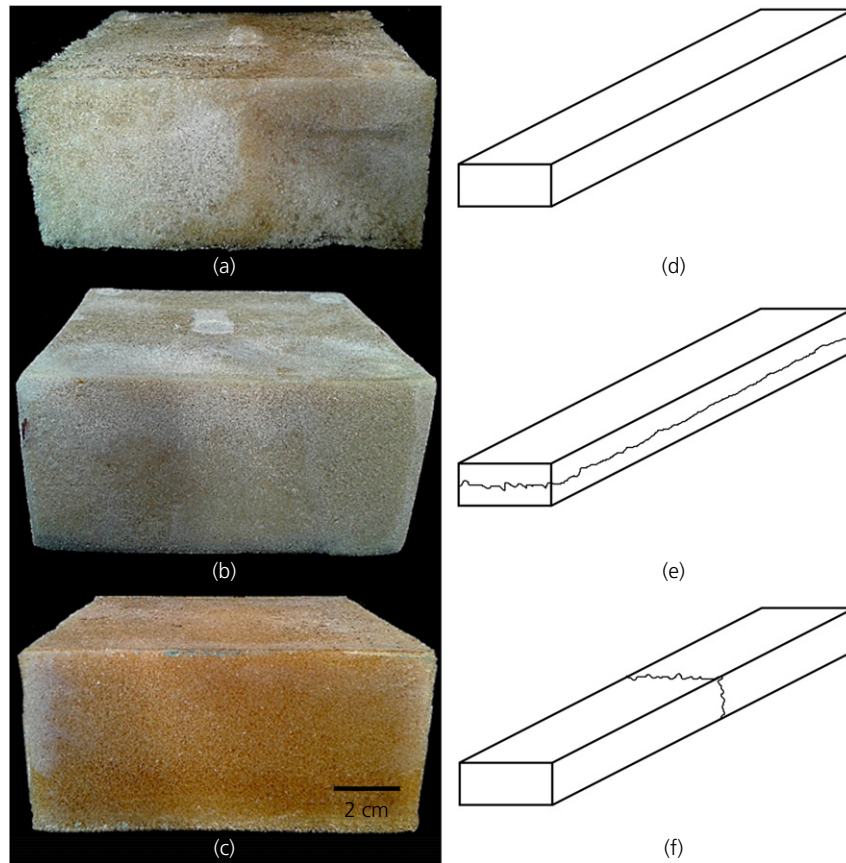Dams, Sareh, Zhang *et al.*

Figure 2. Moulded compressive test specimens of the polyurethane foams: (a) LD40, (b) Reprocell 300, (c) Reprocell 500 and test specimen schematic diagrams (d) one layer, (e) horizontal interface and (f) vertical interface

300 specimens averaged a density of 345 kg/m^3 and expanded significantly less, with a ratio of 2:1. Reprocell 500 had a density averaging 685 kg/m^3 and displayed a minimal expansion of 1·5:1. During specimen creation, the laboratory temperature was 20·3 ± 0·5°C with 52% air humidity ±5%.

2.3 The syringe deposition device

To deposit the foam material autonomously, a motorised syringe device was developed as shown in Figure 3. The device employed a miniature high-power 6 V direct current (DC) brushed motor with a 986:1 metal gearbox (PRE, 2016) powered by a PL155 Aim TTI bench supply. The rotary motion of the motor's shaft was translated to linear motion using a leadscrew mechanism, which moved the plungers of the two syringes simultaneously. Currently, the aerial robot carrying capacity is 0·6 kg, therefore the amount of material capable of being lifted was accommodated by two BD Plastipak 50 ml concentric luer lock syringes. Attached to the luer lock was a mixing device consisting of two 3 mm internal diameter silicone rubber tubes joined to a single 5 mm internal diameter silicone tube with a plastic connector. The single

5 mm tube contained one (for LD40) or two (for Reprocell 300 and 500) 3M 5·3 mm static epoxy mixing nozzles.

The motor was driven at a constant voltage of 5·95 V, thereby allowing the power requirements for the three foams to be determined by the current. With Reprocell 300 and 500, foam deposition on a level surface was attempted with two static mixers, the first followed by 34 cm of tubing (theoretically a 2 min flow duration) and the second, 17 cm (1 min flow duration), to accommodate the different stages of reaction. For the LD40 foam, a single static mixer and a subsequent 17 cm length of 5 mm diameter tubing was used.

The syringe device was suitable for integration into the 3DR ArduCopter Quad aerial robot (as shown in Figure 1) equipped with an ArduPilot on-board processor, three axis accelerometers, three axis magnetometers and four brushless motors with speed controllers. For this study, stationary positioning of the extrusion nozzle was assumed. The deposition of foam on to a free surface served to confirm the feasibility of 3D printing the material, rather than producing the
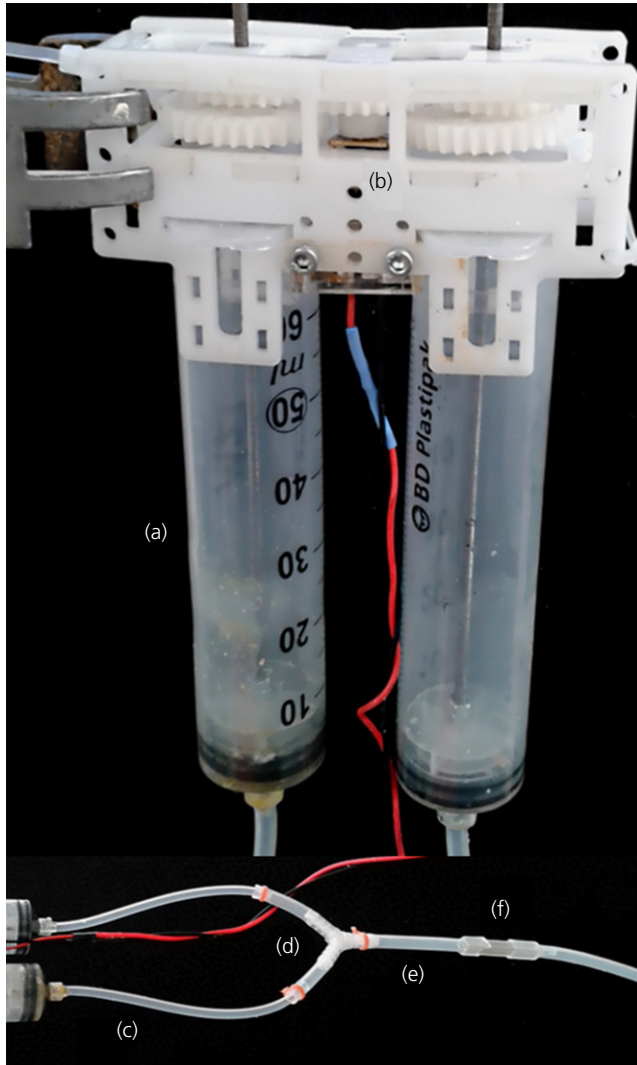
5

Construction Materials
Volume 173 Issue 1

**Aerial additive building manufacturing:
three-dimensional printing of polymer
structures using drones**
Dams, Sareh, Zhang *et al.*

Figure 3. The dual-syringe deposition device and tubing:
(a) concentric luer lock syringes, (b) 6 V DC motor, (c) 3 mm
internal diameter silicone tubing, (d) plastic interconnector,
(e) 5 mm internal diameter silicone tubing, (f) epoxy static
mixer nozzle

rectangular parallelepiped specimens required for British standards mechanical tests.

2.4 Mechanical tests

Three-point bending and compression tests were conducted on cut-edged and moulded specimens in accordance with the rigid cellular plastics standards BS 4370-4:1991 (BSI, 1999) and BS EN ISO 844:2014 (BSI, 2014), respectively. The mechanical properties were tested both parallel and perpendicular to the direction of expansion using a 50 kN Instron Universal 2630-120/305632 for the flexure tests of all three foams, along with LD40 compressive strength tests. An Automax 5 50-C46W2

was used for Reprocell 300 and 500 compressive tests due to a greater force than 50 kN being required.

Deformation due to long-term loading was analysed using a bespoke creep rig (Figure 4), fitted with Solartron LE12 linear encoders (LEs) as optical gauges. The device accommodated eight specimens measuring 30 mm high $\times$ 20 mm $\times$ 20 mm. There were two specimens each of LD40, Reprocell 300 and Reprocell 500 hardened foams (one specimen with a vertical interface and one without an interface) along with a solid pine whitewood timber specimen, perpendicular to the grain direction (a weaker timber) and an oak specimen parallel to the grain (a stronger timber) for comparison. Appropriately sized weights were suspended from the horizontal lever arms at a distance of 630 mm from the specimens (Figure 4). The pivots were 35 mm from the specimens, providing a mechanical advantage of 18. The weights were relative to the average compressive strength of the material at a ratio of 32:1. This corresponded to 1, 0·25 and 0·025 kg for the Reprocell 500, Reprocell 300 and LD40 foams, respectively. The pine specimen was assumed to have a compressive strength >4 MPa and the Oak specimen >8 MPa (WoodworkWeb, 2017), therefore these were conservatively subjected to 0·125 and 0·25 kg, respectively. Steel plates 2 mm thick and measuring 25 mm wide $\times$ 40 mm long was placed on top of the specimens to ensure that force was applied uniformly to each specimen.

The eight Solartron LE12 linear displacement transducers formed an Orbit 3 network with a Solarton USBIM Mk2 USB controller connected to a Solartron PIM supplementary power supply, to ensure power to all eight LEs. Measurements were recorded every 15 min over a period of 14 d. Temperature and humidity were monitored for the duration of the test period to ascertain the effect of differing environmental conditions; these readings were synchronised with the orbit network.

2.5 Rheological tests

The liquid components of the foam – all three resins and the M27 Isocyanate – were tested to determine viscosity using a Bohlin C-VOR 200 rotational Rheometer with torque rebalance software and a temperature controlling water bath. The geometry was of 4°/40 mm specification, with a gap of 150 μm between upper and lower plates. The measurements were controlled by applied shear stresses, which ranged from 0·02 to 20 Pa, with 50 samples taken within the range and a 5 s delay specified between samples. Each liquid was tested three times over the stress range and at temperatures of 26, 30, 34, 38 and 42°C to determine how viscosity changed as temperature increased.

The mixed creamy, viscous liquids of the foams were analysed with a Malvern Kinexus Ultra+ rheometer using a bespoke
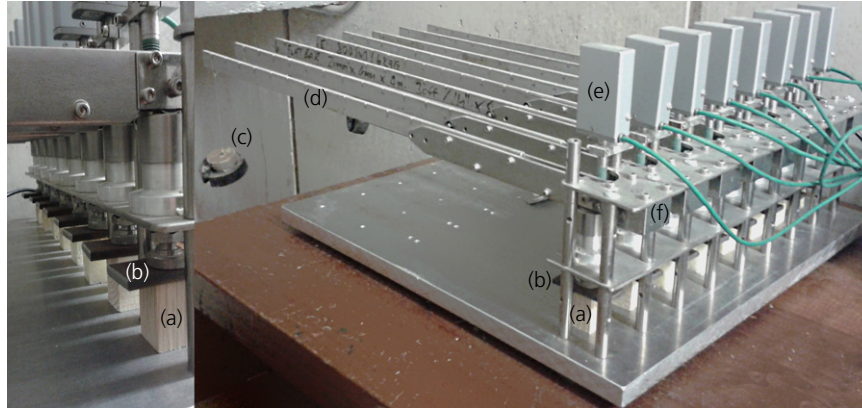
6

Construction Materials
Volume 173 Issue 1

Aerial additive building manufacturing: three-dimensional printing of polymer structures using drones
Dams, Sareh, Zhang *et al.*

Figure 4. The creep rig: (a) cuboid specimens, (b) metal plates to cover the specimens and ensure uniform loading, (c) suspended weights, (d) horizontal lever arms, (e) solar orbit LEs, (f) pivots

method that increased the gap between the geometry and the base plate as the liquid expanded. The diameters of the upper and base disposable plates were 25 and 60 mm, respectively. The gap began at 1 mm; following the recognition of normal force reaching a level of 0·005 Newtons, the method exercised normal force control, maintaining a constant force to avoid compression of the foam and analyse the vertical expansion of the material. The mixed liquids were hand-stirred for 40 s prior to placing them upon the lower disposable plate and oscillatory stress was applied with a flat geometry at a constant shear strain of 0·1. The method recorded the elastic modulus G', viscous modulus G'' and phase angle, δ, over a time period of 9 min to monitor how the rheological properties changed as the mixed foam solidified.

2.6 Microscopy

Two microscopy approaches were utilised to visualise the solid foam. A JEOL SEM6480LV scanning electron microscope (SEM) was used to obtain images of cuboid samples at a magnification of 70×. A 10 nm gold coating was applied to the samples prior to insertion into the electron microscope chamber to reduce charging. In addition, cuboid samples of the three foams were vacuum impregnated with resin and polished. Images were recorded using a Leica M205C stereo optical microscope and the Leica application suite V3·8 software application at 5× magnification. Images were recorded of cut-edged interiors, moulded exteriors and material interfaces.

3. Results

3.1 Mechanical tests

The compressive and flexural strengths of the three different types of foam can be seen in Figure 5. The compressive strength achieved with the hand-mixed Reprocell 500

specimens exceeded 30 MPa, with that of one-layered specimens almost reaching 40 MPa. This is far in excess of the manufacturer's specification (11·7 MPa) (Isothane, 2016b). Reprocell 300 compressive strengths were <10 MPa for specimens with interfaces; however, those of one-layered specimens almost reached 15 MPa. Compressive strengths for LD40 were <1 MPa.

The flexural strength of Reprocell 500 reached 25 MPa, revealing that it is comparable to the lower range of timber, which is 30 MPa (Howard, 2003). However, failure with both Reprocell 500 and 300 was universally brittle, and vertical interface cut-edge specimens (where the direction of expansion was parallel to the applied load) were considerably more fragile and failed to reach 5 MPa. Fragility was not evident in moulded specimens with vertical interfaces, where the direction of expansion was perpendicular to the applied load. The flexural strength results provide an elastic modulus range of <0·1 GPa for LD40, 0·2–0·6 GPa for Reprocell 300 and 0·4–1·4 GPa for Reprocell 500. LD40 displayed ductile failure and the vertical interface moulded specimens, again loaded perpendicular to expansion, performed well in relation to the one-layered and horizontal interface specimens.

Two specimens of each foam were tested in the creep rig. For each foam, the single-layered and vertical interface specimen strengths were consistent, therefore Figure 6(a) shows the mean specimen deformation for each of the three foams. Reprocell 500 and Reprocell 300 performed competitively with oak. As expected, the low-density LD40 was the foam most susceptible to creep. The oak and pine specimens were influenced by environmental conditions and fluctuated significantly (Figure 6(b)); this is particularly evident around 1 and 7 d. The foams were influenced less by temperature and humidity.
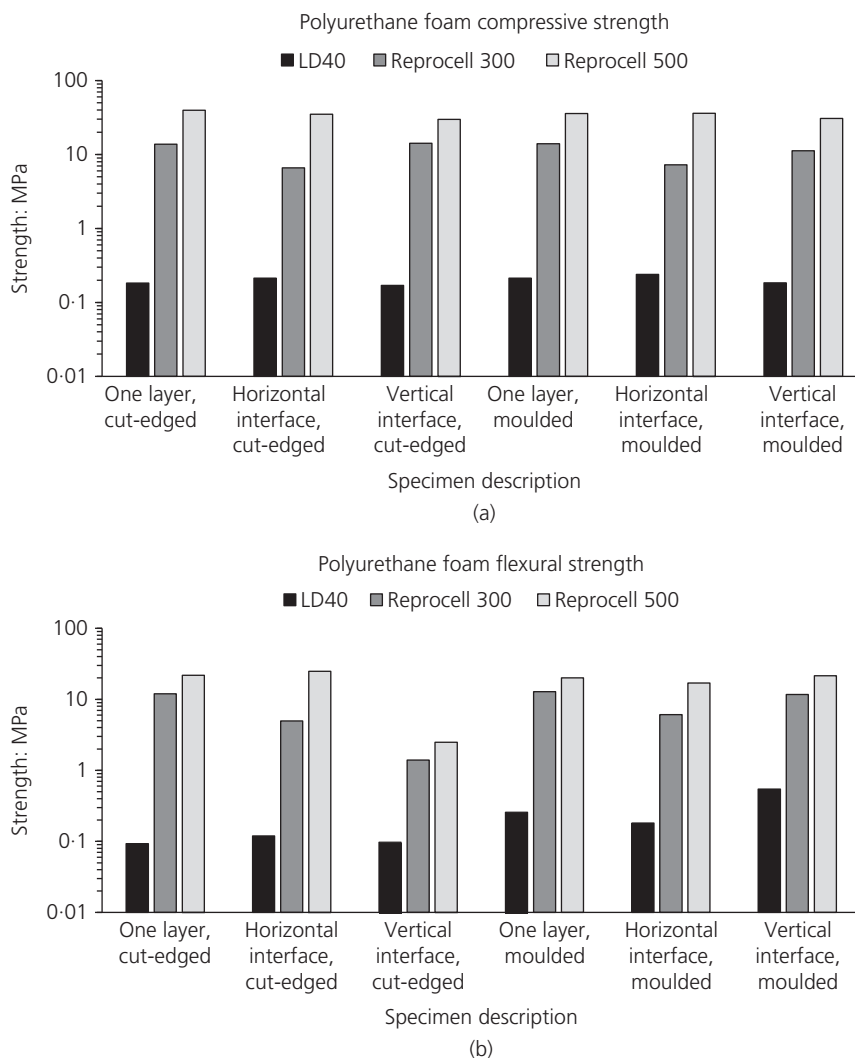
7

Construction Materials
Volume 173 Issue 1

Aerial additive building manufacturing: three-dimensional printing of polymer structures using drones
Dams, Sareh, Zhang *et al.*

Polyurethane foam compressive strength

Polyurethane foam flexural strength

Figure 5. Mechanical test results: (a) compressive strength at fracture or 10% relative deformation, (b) flexural strength at fracture or 0·05 tensile strain

3.2 Power, energy and syringe deposition

Table 1 summarises the energy and power required to draw up and deposit 2 × 50 ml of liquid. This represents the energy and power required for a single aerial robot to obtain and expel its maximum carrying capacity. Through the 5 mm internal diameter tubing, the velocity of liquid foam travel, without expansion, was 17 cm/min. There was negligible variation observed in time between the three types of foam both for drawing up and deposition. The syringe device took 15 min to draw up 2 × 50 ml of liquid, and 15 min to deposit it, operating at a rate of 3·33 ml/syringe/min. The influence of the visibly greater viscosity of the Reprocell foam resin components had been mitigated by prior heating to a temperature of 35 ± 5°C. Reprocell 500 deposition required approximately twice as much energy as LD40.

3.3 Rheology

The rheometer results are presented in Figure 7. All liquid components behaved in a Newtonian manner and experienced a reduction in viscosity as temperature increased (Figures 7(a)–7(d)). At 2000–4000 cP, Reprocell 300 displayed the greatest viscosity. All three mixed foams took ∼9 min to change from liquid-like behaviour, where G'' is dominant, to solid-like behaviour beyond the gelling point where G' becomes dominant. The gelling point was 529 s for Reprocell 500 as shown in Figure 7(e). All mixed foams displayed non-Newtonian behaviour and two distinct peaks with the phase angle, δ; Figure 7(e) shows the phase angle peaks for Reprocell 500. The expansion of the foam was recorded by the normal force control as being 1·9:1 for Reprocell 300 and 1·4:1 for Reprocell 500.

8

Construction Materials
Volume 173 Issue 1

Aerial additive building manufacturing:
three-dimensional printing of polymer
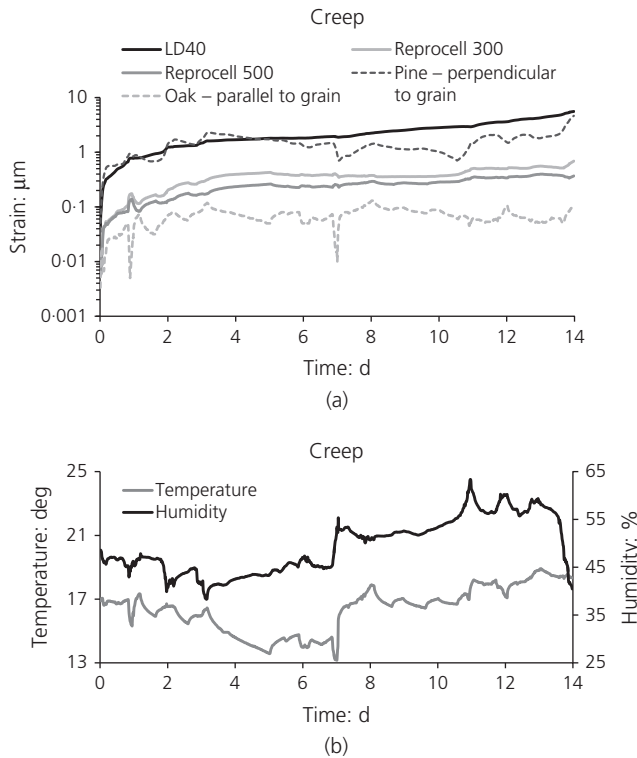structures using drones
Dams, Sareh, Zhang *et al.*

Figure 6. The creep rig results showing deformation due to
long-term loading along with the temperature and humidity data:
(a) foam specimen mean deformation and timber specimen
deformation, (b) temperature and humidity

3.4 Microscopy

The SEM images in Figure 8 highlight the difference in poros-
ity between a moulded specimen exterior (Figures 8(a), 8(c)
and 8(e)) and a cut-edge specimen (Figures 8(b), 8(d) and 8(f)).
The exterior image of Reprocell 500 shows an absence of
pores at the specified magnification. Material interfaces can be
seen running horizontally across Figure 8(g) (LD40) and
Figure 8(h) (Reprocell 500). Optical microscope images can be
seen in Figure 9. The image of an interface within a Reprocell
500 sample shows reduced pore sizes along the edge of the
upper layer (Figure 9(d)). Reprocell 500 exhibited greater
variation in cell size than the more uniform Reprocell 300. The
Reprocell 500 resin component has a lower viscosity, which

makes formation of microcells easier, resulting in uneven diam-
eter sizes and larger cells being present (Zhang *et al.*, 2014).

4. Discussion

The high compressive strength of the moulded specimens of
Reprocell 500 was aided by its high density and low expansion
ratio. The average density (685 kg/m^3) was the result of exten-
sive and rigorous hand-mixing before, during and immediately
following polymerisation. The compressive strengths of the
cut-edge specimens were similar to those of the moulded speci-
mens. The SEM images show significant closed porosity at the
moulded edges (Figures 8(a), 8(c) and 8(e)), yet the presence of
a significant edge effect enhancing the compressive strength of
the material is not evident in one layered, horizontal interface
or vertical interface specimens.

Moulded specimens with a vertical interface far outperformed
cut-edge vertical specimens in flexure. However, it is reasoned
that this gap in performance is due to the stronger adhesion of
a vertical interface formed by the pouring of liquid perpen-
dicular to the direction of loading, rather than the edge effect
of the moulding.

LD40 exhibited ductile failure in flexural tests. The interface
between two layers, intuitively expected to be a weakness,
revealed itself to be an area of strength within the material,
with specimens containing vertical interfaces not cracking at
the interface during flexural tests, but elsewhere within the
single layer of the rest of the specimens. Likewise, the horizon-
tal interface provided extra resistance in three-point bending,
contributing to a gradual failure with warning cracks rather
than catastrophic failure. However, LD40 specimens possessed
a bending strength of <1 MPa, suggesting suitability for non-
structural purposes.

The ductile failure of LD40 contrasted with the brittle failure
of the Reprocell foams in flexure, where vertical interfaces
parallel to the expansion of the foam in cut-edged specimens
did indeed prove to be a weakness, as flexural specimens
cracked predominantly at the interface and did not match the
performance of one-layered or horizontal interfacial specimens.
Reprocell 500 is comparable to timber in terms of flexural
strength, but it is less stiff; the modulus of elasticity is
a maximum of 1·4 GPa. This is similar to timber's elastic

Table 1. Power and energy consumption of the syringe device for the three foams

Foam	Voltage: V	Current ± 5 A: A	Time: s	Energy: J	Charge: C	Power: W	Energy transferred/number of units: kWh
LD40	5·95	0·030	1800	321	54	0·179	0·0000893
Reprocell 300	5·95	0·040	1800	428	72	0·238	0·000119
Reprocell 500	5·95	0·055	1800	589	99	0·327	0·0001636

Construction Materials
Volume 173 Issue 1

Aerial additive building manufacturing:
three-dimensional printing of polymer
structures using drones
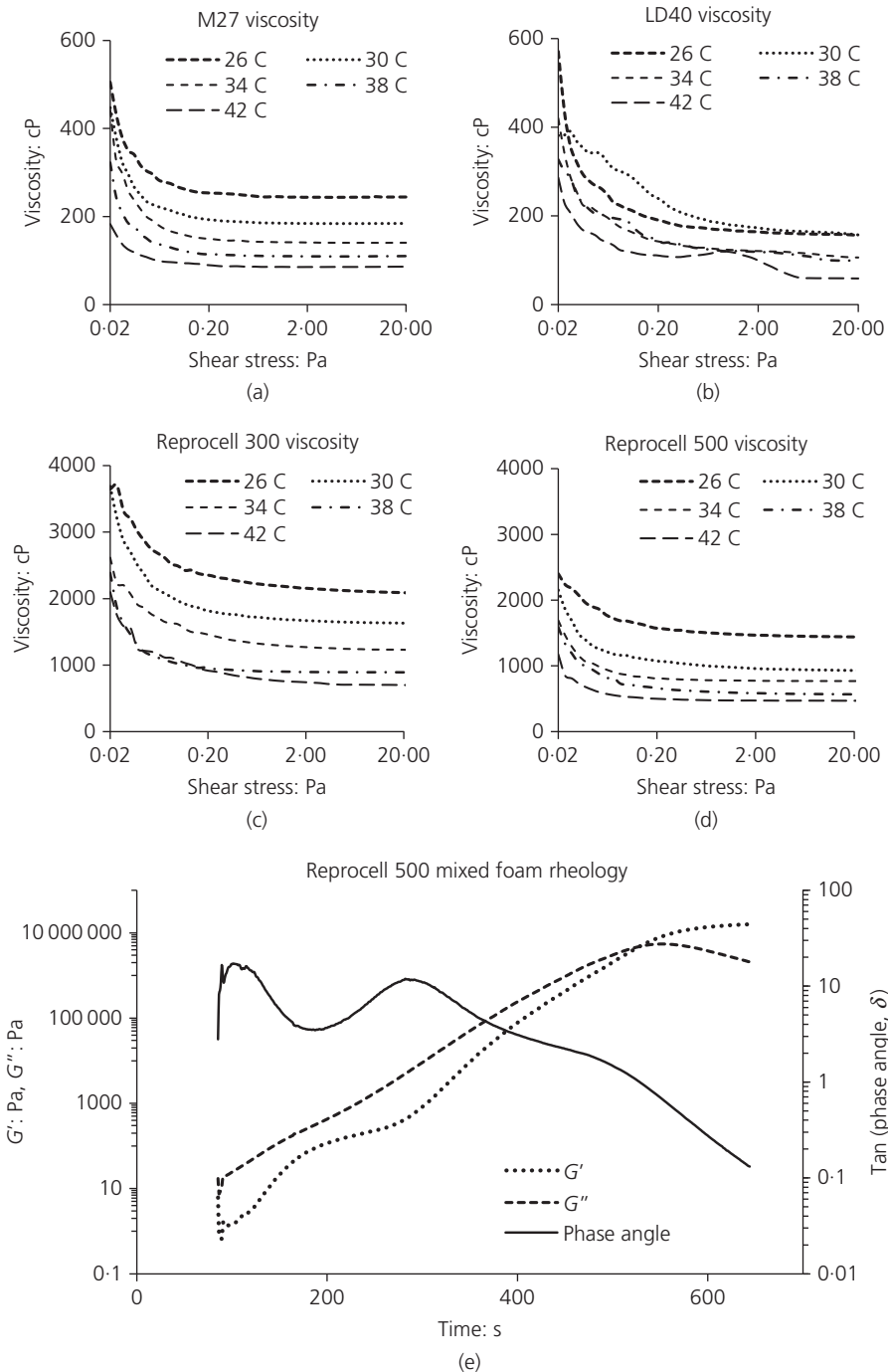Dams, Sareh, Zhang et al.

Figure 7. The rheometer test results showing (a) – (d) the viscosity of the three foam resins and M27 Isocyanate hardening agent liquid components. Note the different y-axis for (a) and (b) and (e) the rheology of the mixed Reprocell 500 liquid: elastic modulus (G′), viscous modulus (G″) and the phase angle (δ) plotted against time

modulus in the weaker axis perpendicular to the grain rather than parallel to the grain, which can be as high as 20 GPa (Howard, 2003). The SEM images show a material that is not

homogeneous; the pores differ greatly in size and distribution. The interfaces in Figures 8(g) and 8(h) show a clear difference – the LD40 layers have a superior, seamless bond, while the
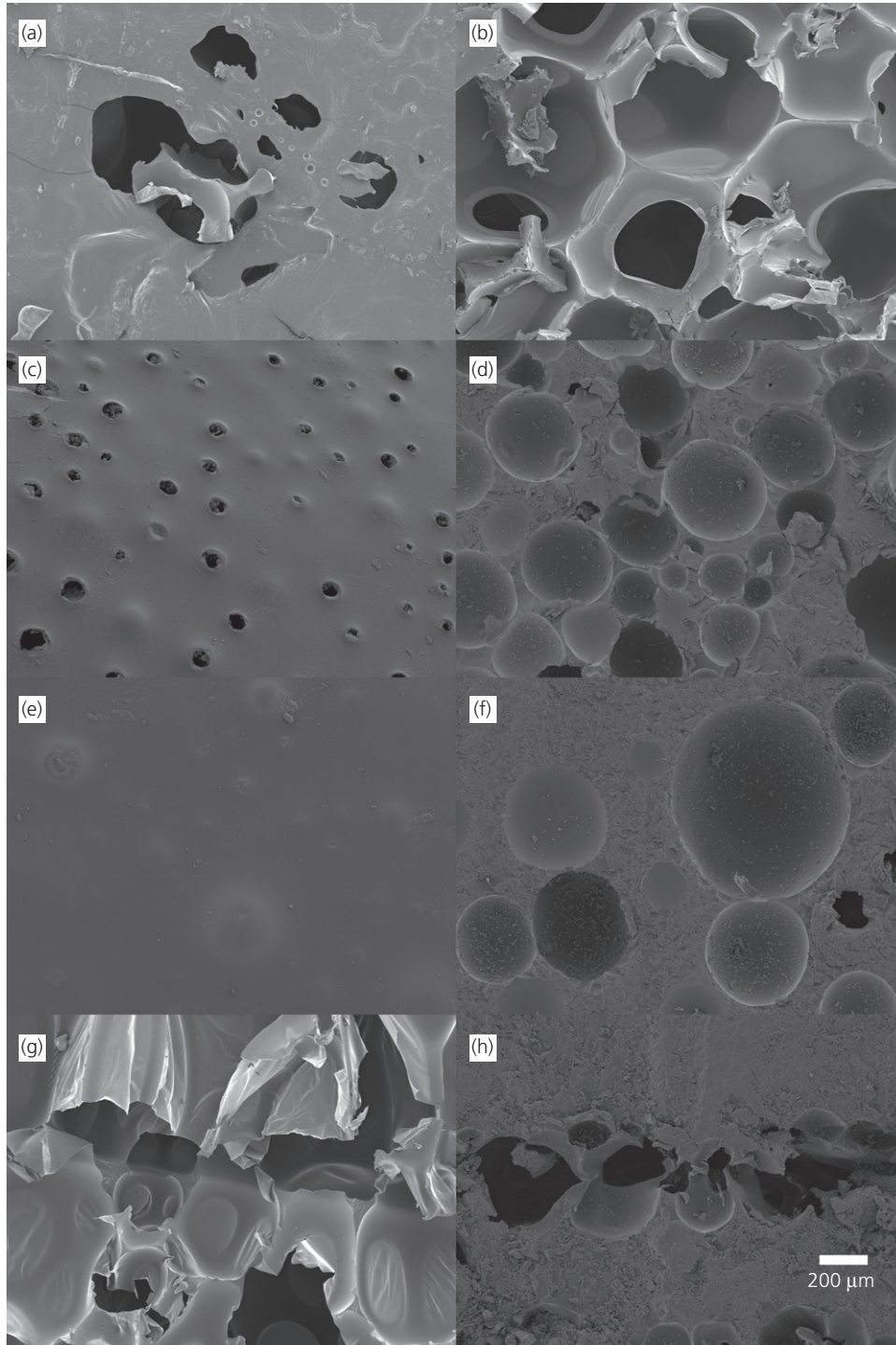
Construction Materials
Volume 173 Issue 1

Aerial additive building manufacturing:
three-dimensional printing of polymer
structures using drones
Dams, Sareh, Zhang *et al.*

Figure 8. SEM images taken at 70×: (a) LD40 moulded edge, (b) LD40 cut-edge, (c) Reprocell 300 moulded edge, (d) Reprocell 300 cut-edge, (e) Reprocell 500 moulded edge, (f) Reprocell 500 cut-edge, (g) LD40 interface, (h) Reprocell 500 interface
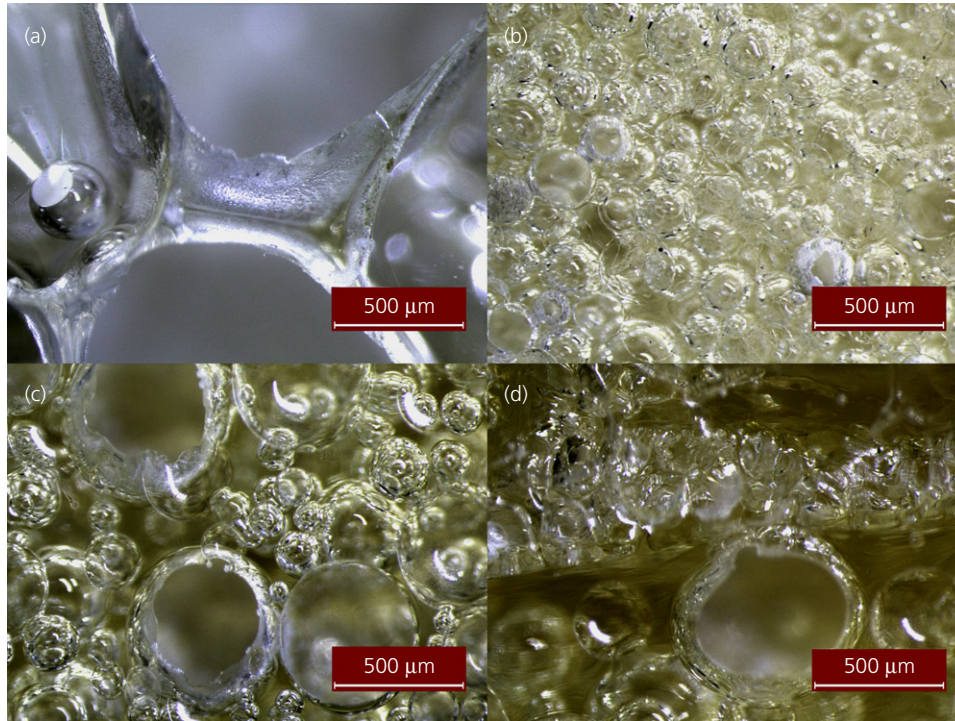
Construction Materials
Volume 173 Issue 1

Aerial additive building manufacturing: three-dimensional printing of polymer structures using drones
Dams, Sareh, Zhang *et al.*

Figure 9. Stereo optical microscopy images taken at 5×: (a) LD40 cut-edge, (b) Reprocell 300 cut-edge, (c) Reprocell 500 cut-edge, (d) Reprocell 500 interface

Reprocell 500 dense foam material surrounds a distinct line of pores where the layers meet. The deposition of a small amount of material in situ by an aerial robot would result in vertical interfaces. This could be mitigated by a sequence of aerial robots immediately depositing their fluid before the preceding fluid had set, minimising each printed layer to one vertical interface at differing locations. Lateral/wind loading would be a secondary concern, as this would impart loading perpendicular to the rise of the foam. Reprocell 500 represents a viable proposition as a compressive element in a 3D printed structural solution and LD40 a viable insulating material.

The compressive viability of Reprocell 500 is further emphasised by the creep results (Figure 6). Reprocell 500 is competitive with oak and the Reprocell 500 specimens were subjected to a heavier weight. It is entirely possible that the oak specimen, parallel to the grain, had a compressive strength equivalent to or greater than that of Reprocell 500 and would have deformed to a greater extent with a 1 kg weight. The timber specimens showed clear expansion with increased humidity and contraction with decreased humidity, whereas the Reprocell foams were significantly more stable and resistant to environmental change. Reprocell foams are suitable to resisting deformation from long-term loading.

With the rheology results in Figure 7, it can be seen that with all four fluids, the polymer chains have greater freedom to slide past each other as both shear stress and temperature increase, leading to reduced viscosity. The heating of the liquid components of Reprocell 300 and Reprocell 500, and the subsequent reduction in viscosity, contributed to the amount of power being required to draw-up and deposit the Reprocell foams being less than double than that required for LD40 (Table 1). Considering that Reprocell 500 has order-of-magnitude compressive and flexural strengths superior to the LD40 foam, the extra energy is justified. The mixed fluids used in the rheology tests experienced considerably less rigorous hand mixing than the mechanical test specimens due to the logistical requirements of placing and suitably trimming the samples. Tests confirm initial liquid-like behaviour, followed by a reduction in the phase angle as viscosity increases. This is followed by confirmation that the darkening, 'thinning' of the liquid as polymerisation occurs results in reduced viscosity and a second clear peak as the mixed foam again becomes more liquid like (Figure 7(e)).

The final phase of solidification in the rheometer tests took almost three times as long as for the hand-mixed specimens. Mixed Reprocell foams deposited by the syringe device also

Construction Materials
Volume 173 Issue 1

Aerial additive building manufacturing:
three-dimensional printing of polymer
structures using drones
Dams, Sareh, Zhang *et al.*

did not react fully within the 3 min hand-mixed timeframe, as the static mixers in the tubing supplied less rigorous mixing than was achieved by hand. The polymerisation stage of the Reprocell foams' chemical reaction did not take place inside the tubing, but instead post-deposition, after lateral spreading on the free surface had occurred with negligible vertical expansion. Clearly, as the stress applied to the mixed Reprocell foams increased, the rate of reaction increased. LD40 syringe device deposition resulted in the material reacting and expanding exactly as the hand-mixed samples did; however, expansion on the free surface varied greatly in magnitude and direction, which is undesirable for the given context.

The realisation of 3D printed hardened specimens on a free surface with sufficient shear strength and yield stress to support further layers is a challenge and will involve modifying the rheology of the foam, for example by adding solid particles to increase the shear strength. Two approaches may be investigated further with the syringe deposition device; more rigorous mixing, whether by larger static mixers or introducing mechanical mixers, or increasing the tubing length and introducing more static mixers at intervals, so that the liquid may stay within the device for a longer period. The former approach would be preferable to increase the pace of deposition in a construction environment and allow aerial robots to deposit liquid at a greater rate.

This study shows that high-density polyurethane foam could feasibly be used as a structural polymeric material. It also demonstrates that a small dual-syringe device light enough to be carried by a quadcopter is capable of depositing and mixing liquids of varying viscosities while maintaining the mixing ratio required for polymerisation. The potential contribution to the construction industry of aerial additive building manufacturing is significant. In addition to reducing labour costs, mitigating health and safety issues and reducing waste by using material efficiently, the aerial approach would release autonomous construction from ground-based design and logistical size restrictions. It would facilitate both building repair work involving inaccessible or inhospitable locations, where human labour may be compromised both in terms of accuracy and safety, and the autonomous creation of structures upon unfavourable terrain and under hostile conditions unsuitable for heavy, grounded machinery.

5. Conclusions

It is concluded that Reprocell 500 high-density foam has the potential to be both a homogeneous structural material and, particularly, a compressive element in a composite structural solution 3D extrusion printed by aerial robots. The ability to be printed by an autonomous device requires modification of the foams' rheology to achieve high viscosity immediately after

extrusion and provide sufficient shear strength to support further layers while still liquid. This challenge is being investigated by the authors, using particle addition and active mixing. LD40 has the potential to be 3D extrusion printed for non-structural purposes such as insulation. All three foams were successfully drawn-up, mixed and deposited by a single motor dual-syringe deposition device. By investing approximately twice as much power and energy, the syringe device was capable of depositing material in excess of ten times higher density and with compressive and flexural strengths an order of magnitude higher. The study has demonstrated the feasibility of 3D extrusion printing a polymeric structural material using an aerial robot.

REFERENCES

Alaa MA, Yusoh K and Hasany SF (2015) Pure polyurethane and castor oil based polyurethane: synthesis and characterization. *Journal of Mechanical Engineering and Sciences (JMES)* **8**: 1507–1515, http://dx.doi.org/10.15282/jmes.8.2015.25.0147.

BSI (1991) BS 4370-4: Methods of test for rigid cellular materials, Method 14 – Determination of flexural properties. BSI, London, UK.

BSI (2014) BS EN ISO 844: Rigid cellular plastics – Determination of compression properties. BSI, London, UK.

Frearson A (2016) *DUS Architects Builds 3D-Printed Micro Home in Amsterdam.* Dezeen Limited, London, UK. See http://www.dezeen.com/2016/08/30/dus-architects-3d-printed-micro-home-amsterdam-cabin-bathtub/ (accessed 03/01/2017).

Howard S (2003) *Materials Data Book 2003 Edition.* Cambridge University Engineering Department, Cambridge, UK.

Hunt G, Mitzalis F, Alhinai T, Hooper PA and Kovac M (2014) 3D printing with flying robots. *Proceedings of International Conference on Robotics and Automation, Hong Kong.* Institution of Electrical and Electronics Engineers (IEEE), Piscataway, NJ, USA, pp. 4493–4499.

Isothane (2016a) *The Reprocell Range.* Isothane, Accrington, UK. See http://www.isothane.com/prod/reprocell-range/ (accessed 17/11/2016).

Construction Materials
Volume 173 Issue 1

**Aerial additive building manufacturing:
three-dimensional printing of polymer
structures using drones**
Dams, Sareh, Zhang *et al*.

Isothane (2016b) LD40. Isothane, Accrington, UK. See http://www.
isothane.com/prod/ld40/ (accessed 10/11/2016).

Kreiger MA, MacAllister BA, Wilhoit JM and Case MP (2015) The current
state of 3D printing for use in construction. *Proceedings of the
2015 Conference on Autonomous and Robotic Construction of
Infrastructure, Ames, IA, USA*. Iowa State University Digital
Repository, Iowa, USA, pp. 149–158.

Labonnote N, Rønnquist A, Manum B and Rüther P (2016) Additive
construction: state-of-the-art, challenges and opportunities.
Automation in Construction **72**: 347–366, https://doi.org/10.1016/
j.autcon.2016.08.026.

Le TT, Austin SA, Lim S *et al.* (2012) Hardened properties of
high-performance printing concrete. *Cement and Concrete
Research* **42(3)**: 558–566.

Lim S, Buswell RA, Le TT *et al.* (2012) Developments in construction-
scale additive manufacturing processes. *Automation in Construction*
21: 262–268, https://doi.org/10.1016/j.autcon.2011.06.010.

PRE (Pololu Robotics and Electronics) (2016) *Micro Metal Gearmotors.*
Pololu Robotics and Electronics, Las Vegas, NV, USA. See
http://www.pololu.com/category/60/micro-metal-gearmotors
(accessed 24/01/2017).

Schutte K, Sahli H, Schrottmayer D *et al.* (2001) ARC: a camcopter based
mine field detection system. In *Presented at the Fifth International
Airborne Remote Sensing Conference*. Environmental Research
Institute of Michigan, Ann Arbor, MI, USA, vol. 17, p. 20.

Siciliano B and Khatib O (2008) *Springer Handbook of Robotics.*
Springer International Publishing, New York, NY, USA.

Stansbury JW and Idacavage MJ (2016) 3D printing with polymers:
challenges among expanding options and opportunities. *Dental
Materials* **32(1)**: 54–64.

Sugiura R, Noguchi N, Ishii K and Terao H (2003a) Development of remote
sensing system using an unmanned helicopter (part 1). *Journal of
the Japanese Society of Agricultural Machinery* **65(1)**: 53–61.

Sugiura R, Fukagawa T, Noguchi N *et al.* (2003b) Field information
system using an agricultural helicopter towards precision farming.
In *Advanced Intelligent Mechatronics, 2003. AIM 2003.
Proceedings of 2003 IEEE/ASME International Conference,
Wageningen, the Netherlands* (van Henten EJ, Goense D and
Lokhorst C (eds)), pp. 1073–1078.

Trovati G, Sanches EA, Neto SC, Mascarenhas YP and Chierice GO (2010)
Characterization of polyurethane resins by FTIR, TGA, and
XRD. *Journal of Applied Polymer Science* **115(1)**: 263–268.

WoodworkWeb (2017) *Wood Strengths.* WoodworkWeb, Canada. See
http://www.woodworkweb.com/woodwork-topics/wood/146-wood-
strengths.html (accessed 10/01/2017).

Wright S (2005) Uavs in community police work. In *Infotech@
Aerospace*. American Institute of Aeronautics and Electronics
(AIAA), Reston, VA, USA, p. 6955.

Wu L, Van Gemert J and Camargo RE (2012) *Rheology Study
in Polyurethane Rigid Foams*. Huntsman International
LLC, The Woodlands, TX, USA.

Zhang L, Ding X and Ou Y (2014) Properties of rigid polyurethane
foams prepared with synthesized PIPA polyol. *American Journal of
Chemistry and Application* **1(1)**: 7–14.

How can you contribute?

To discuss this paper, please email up to 500 words to the editor at journals@ice.org.uk. Your contribution will be forwarded to the author(s) for a reply and, if considered appropriate by the editorial board, it will be published as discussion in a future issue of the journal.

Proceedings journals rely entirely on contributions from the civil engineering profession (and allied disciplines). Information about how to submit your paper online is available at www.icevirtuallibrary.com/page/authors, where you will also find detailed author guidelines.